Structural and Impedance Studies on Chemically Synthesized Lead-Oxide Nanoparticles Doped with Mn²⁺ and S²⁻

[1]S. Abarna , [2]R. Muthumariammal, [3]H. Sindhu Lakshmi and [4]J. Juliet Latha Jeyakumari
[1,2,3]Scholar, [4]Assistant Professor,
[1,2,3,4]Department of Physics, Sarah Tucker College, Tirunelveli, Tamilnadu, India.

Abstract-- Lead oxide nanoparticles doped with Mn²⁺ and S²⁻ were synthesized by Solvothermal method using lead acetate and urea as precursor. The obtained samples were characterized by XRD and Impedance studies. The average size of the prepared samples were determined using X-ray diffraction pattern and it was found to be 55nm for pure PbO, 30 nm for doped with Mn²⁺ and 45nm for S²⁻. The electrical response was studied by impedance complex spectroscopy over a broad frequency range (1–1 MHz) at room temperature and it indicated the electrical properties of the materials are strongly dependent on frequency.

Key Words-- *Nanoparticles, Lead oxide, Solvothermal method, Impedance Spectroscopy*

I. INTRODUCTION

In recent years, the synthesis of nanomaterials is an important research in the various scientific and industrial fields. The properties of such materials are novel and can be engineered by controlling the dimensions of these building blocks and their assembly via physical, chemical or biological methods [1]. Nowadays the unique properties of nanomaterials have motivated the researchers to develop many simpler and inexpensive techniques to produce nanostructures of technologically important materials. Several metal oxide nanoparticles are produced with possible future applications [2–6]. The lead element has many oxide forms including PbO, Pb_2O_3, Pb_3O_4, and PbO_2. Due to their unique properties, lead oxides have wide applications such as network-modifiers in luminescent glassy materials, pigments, gas sensors, paints, storage batteries like lead acid, valve regulated lead acid batteries and lithium secondary batteries and nanoscale electronic devices. Also doping is a well-known approach to modulate the electronic and optical properties of nanoparticles In this work, we report the synthesize of lead oxide nanoparticles and lead oxide doped with Mn^{2+} and S^{2-} using solvo thermal method. The structural and the electrical response are studied.

II. EXPERIMENTAL

A. Materials

Lead oxide $(Pb(C_2H_3O_2)_2)$, Urea (CH_4N_2O), Ethelyne glygol($C_2H_6O_2$), Manganese acetate $(C_6H_9M_nO_{6\cdot2}(H_2O))$ and Sulphur were purchased from Merck Chemical Company and used without further purification. Deionized distilled water was used to prepare all solutions.

B. Instrumentation

A microwave oven with 1000 W power (Butane) was used. Powder X-ray diffraction (XRD) patterns of prepared samples were recorded by diffractometer (XPERT-PRO) using a Cu Kα radiation (λ=1.54Å). The complex impedance study was performed using the impedance analyzer Solatron1260.

C .Synthesis of Samples

Lead acetate and urea were taken in different molecular ratio and were mixed in ethylene glycol and kept in a domestic microwave oven. Microwave irradiation was carried out till the solvent was evaporated completely. The colloidal precipitate was then cooled and washed several times with distilled water and with acetone to remove the organic impurities present if any. The sample was then dried and collected as yield.

Required amount of Manganese acetate and Sulphur were added for the doping of Mn^{2+} and S^{-2} respectively to the above solution and the same procedure was repeated.

III. RESULTS AND DISCUSSION

A. XRD Analysis

The X-ray diffraction pattern was recorded by using Cu Kα radiation (1.5406 Aᵒ). The intensity data were collected over a 2θ range of 20ᵒ - 80ᵒ. The formation of nanostructure lead oxide and Mn^{+2} and S^{-2} doped Lead Oxide were studied using X-ray diffraction (XRD) and the XRD patterns are shown in figures1, 2 and 3 respectively.

The phase purity of the prepared tetragonal nano PbO cube is clearly seen and all diffraction peaks are perfectly indexed to the tetragonal PbO structure [7]. The broadening of the peaks indicated that the particles were   of nanometer scale. The peaks at angles (2θ) around 28°, 35°, 45°, 48° and 59° correspond to the reflection from 101, 002, 102, 112 and 202 crystal planes, respectively [8].
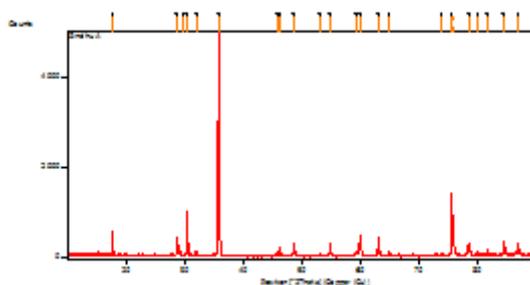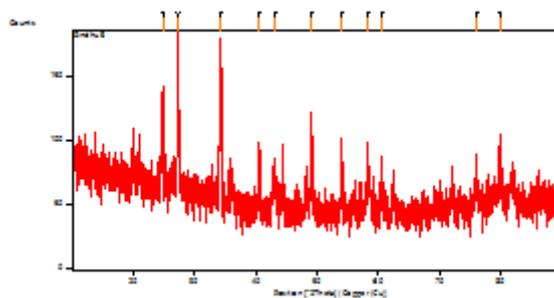

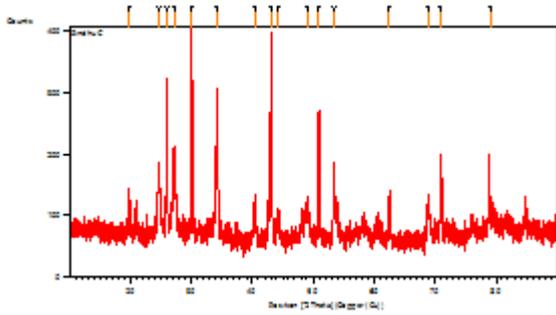Figure 1: XRD of Pure PbO

Figure 2: XRD of Mn⁺² doped PbO

Figure 3: XRD of S^{-2} doped PbO

a. Grain size

The average grain size (D) of the synthesized particles is determined using Debye-Scherrer formula (equation 1)[9, 10].

$$D = \frac{0.9\,\lambda}{\beta\,\cos\theta} \quad \text{------ (1)}$$

Where λ is the wavelength (Cu Kα), β is the full width at the half-maximum (FWHM) of the PbO and θ is the diffraction angle. The grain size was found to be in the range of 38-93 nm for PbO nanoparticle, 14-28 nm for Mn^{+2} doped PbO nanoparticle and 14-57 nm for S^{-2} doped PbO nanoparticle and the values are tabulated in table 1.

b. Dislocation Density

Table 1: XRD Parameters grain size and dislocation density of the samples

Sample	Position 2θ (deg)	FWHM β x 10⁻³ (radian)	Grain size D (nm)	Dislocation Density ρ x 10¹⁴ m⁻²
PbO	28.5787	2.3340	57	3.0191
	35.6410	1.4757	93	4.2496
	48.5784	3.5011	38	6.7806
	54.7054	1.5002	89	1.2472
	62.9803	1.5676	88	6.3162
Mn^{+2} with PbO	27.2097	4.6681	28	1.2718
	34.1840	5.8368	23	1.8836
	40.4781	4.6681	28	1.2076
	49.0525	4.6681	28	1.2076
	53.9580	4.6681	28	1.2076
	58.2895	9.338	14	4.8326
S^{-2} with PbO	27.2757	9.3066	14	4.799
	30.0930	2.2671	51	3.8276
	34.1591	2.3201	57	2.9831
	43.0459	2.6271	51	3.8248
	50.9670	2.3340	57	3.0191
	70.9665	5.8369	23	1.8880

The dislocation density is defined as the length of dislocation lines per unit volume of the crystal [11]. In materials science, a dislocation is a crystallographic defect, or irregularity, within a crystal structure. The presence of dislocations strongly influ-

ences many of the properties of materials. Mathematically, dislocations are a type of topological defect. The dislocation density increases with plastic deformation, a mechanism for the creation of dislocations must be activated in the material. Three mechanisms for dislocation formation are formed by homogeneous nucleation, grain boundary initiation, and interface the lattice and the surface, precipitates, dispersed phases, or reinforcing fibers. The movement of a dislocation is impeded by other dislocations present in the sample. Thus, a larger dislocation density implies a larger hardness [12].

The dislocation density was calculated using the given formula (equation 2) and the values are tabulated in table 1.

$$\rho = \frac{1}{D^2} \quad \text{------- (2)}$$

Where ρ is dislocation density and D is the crystallite size [13].

B. Complex Impedance Analysis

Figures 4, 5 and 6 show the complex impedance spectra (Nyquist plot) of lead oxide nanoparticles, PbO doped with Mn^{+2} and S^{-2} respectively. The graphs show that there is an inclined straight line in the lower frequency range followed by the semi circular arc at higher frequency region and there is an intercept on the real axis. The reason is the grains boundaries are effective in high frequency region, while the grain boundaries are effective in low frequency region, the semicircle appearing in the high frequency region corresponds to grain contribution while in the low frequency region corresponds to the grain boundary contribution [14, 15]. The arc's intercept on the real axis for semicircular gives the value of bulk resistance (R_b) which is increasing with the doping of Mn^{+2} and S^{-2}.
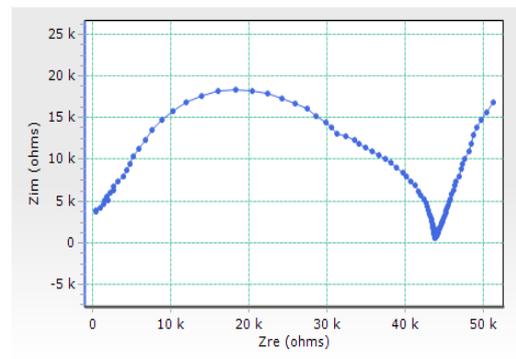

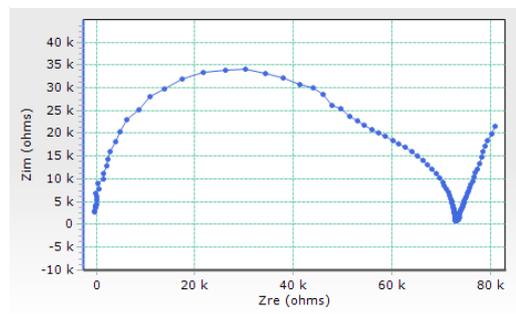Figure 4: Complex impendence spectra of pure PbO

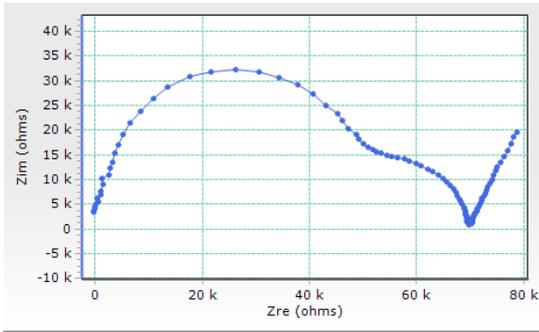Figure 5: Complex impendence spectra of PbO doped with Mn^{+2}

Figure 6: Complex impendence spectra of PbO doped with S^{-2}

The variation of total impedance |Z| with frequency is shown in Figs 7, 8 and 9 for all the samples. It has been observed that |Z| decreases with the increase in frequency for all the compositions. Generally, grain boundaries which are resistive in nature are active at low frequencies, that is why resistance is high in low frequency region, while grains which are conductive in nature are active in high frequency region due to which |Z| is small at high frequencies
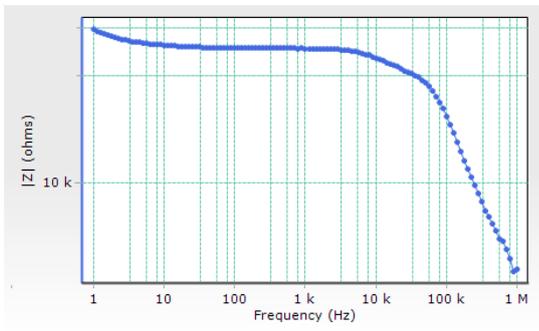

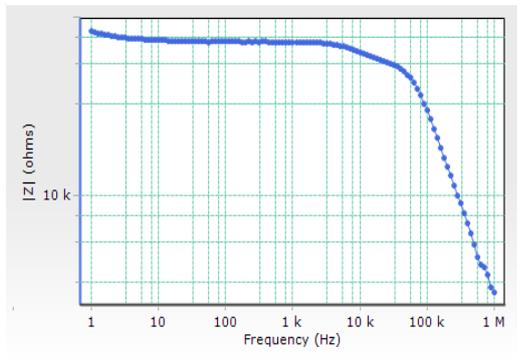Figure 7: Variation of impendence with frequency for pure PbO

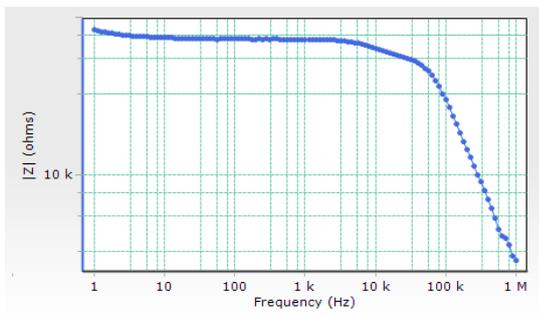Figure 8: Variation of impendence with frequency for PbO doped with Mn^{+2}

Figure 9: Variation of impendence with frequency for PbO doped with S^{-2}

C. V-I Characteristics

The voltage current characteristics of PbO and PbO doped with Mn^{+2} and S^{-2} are shown fig. 10, 11and 12 respectively. It is clear from the graphs that there is a linear relation between current and voltage. This indicates the ohmic nature; there is ohmic contact between samples and electrodes. Ding et al (2008) have also reported the linear relation between current and voltage for CdS nanoparticle [18]. From the slope it is observed that the resistance is large when the potential is low and the resistance becomes low when the potential is high.
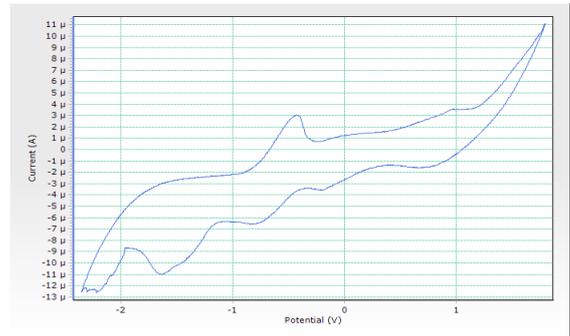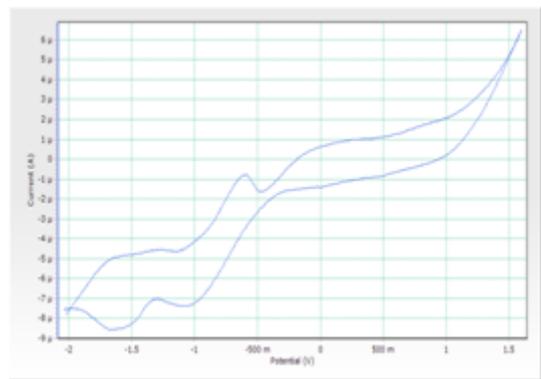

Figure 10: V-I Characteristics of pure PbO

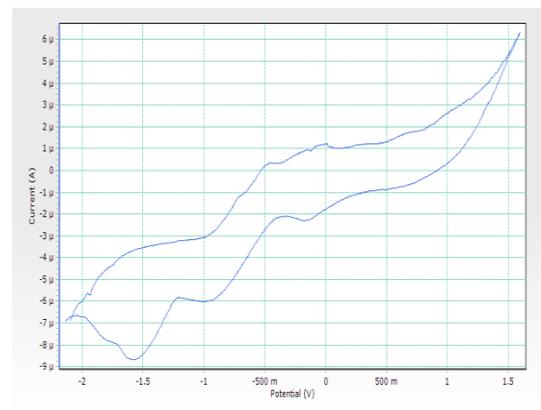Figure 11: V-I Characteristics of PbO doped with Mn^{+2}

Figure: 12 V-I Characteristics of PbO doped with S^{-2}

CONCLUSION

Lead oxide nanoparticle and PbO, Mn^{+2} and S^{-2} doped PbO were prepared by the simple solvothermal method using a microwave oven and the prepared samples were characterized by XRD, and impendence analysis. XRD reveals that the grain size of the prepared samples is in the range of 38-93nm for PbO nanoparticle, 14-28 nm for PbO nanoparticle doped with Mn^{+2} , 14-57 nm for PbO nanoparticle doped with S^{-2}. Complex impedance analysis indicates that the electrical properties of the materials are strongly dependent on frequency. Analysis of this spectra permits to estimate the grain boundary. V-I characteristics infers that is a ohmic contact between the samples and electrodes.

References

[1] Manoj Singh, Manikandan, S., and A.K. Kumaraguru, Nanoparticles: A New Technology with Wide Applications. Res. J. Nanosci. and Nanotech, (2011) 1: 1-11.

[2] F. Nastase, I. Stamatin, C. Nastase, D. Mihaiescu, Prog. Solid State Chem. (2006) 34 :191.

[3] S.H. Yoon, J.S. Kim, Y.S. Kim, Curr. Appl. Phys. 6S1 (2006) e154.

[4] Y.Q. Huang, L. Meidong, Z. Yike, L. Churong, X. Donglin, L. Shaobo, Mater. Sci. Eng. B 86 (2001) 232.

[5] Z. Wang, S.K. Saxena, Solid State Commun. 118 (2001) 75.

[6] H. Gong, J.Q. Hu, J.H. Wang, C.H. Ong, F.R. Zhu, Sens. Actuators B 115 (2006) 247.

[7] Irshad A, Wani A, Ganguly JA, Ahmad T Silver nanoparticles: Ultrasonic wave assisted synthesis, optical characterization and surface area studies. Mater. Lett. 2011; 65(3): 520-522.

[8] Das R, Nath SS, Chakdar D, Gope G, Bhattacharjee R. Preparation of Silver Nanoparticles and their Characterization. J.Nanotech.Online.(2009) 5: 1-6

[9] Nath, S.S., Chakdar, D., and G. Gope, Synthesis of CdS and ZnS quantum dots and their applications in electronics. Nanotrends, (2007)02(03): 1-5.

[10] Dash, P.K. and Y. Balto, Generation of Nano-copper Particles through Wire Explosion Method and its Characterization. Res. J. Nanosci. And Nanotech, (2011)1: 25-33.

[11] Nehru.L C, SwaminathanV, Sanjeeviraja . C .Photo luminescence Studies on Nanocrystalline Tin Oxide Powder for Optoelectronic Devices. American J.Mat.Sci. (2012) 2(2): 6-10.

[12] Sirdeshmukh DB, Sirdeshmukh L, Subhadra KG. Micro- and Macro-Properties of solids: Thermal, Mechanical and Dielectric properties. Springer, NewYork.(2006) ISBN: 9783540317852.

[13] Velumani S, Mathew X, Sebastian PJ, Narayandass Sa K, Mangalaraj D. Structural and optical properties of hot wall deposited CdSe thin films. Solar Energy Materials & Solar cells,(2003) 76(3): 347-358.

[14] Ridha Bellouz, Sami Kallel, Kamel Khirouni, Octavio Pena, Mohamed Oumezzine, Structural, electrical conductance and compleximpedance analysis of $(Nd_{1-x}Cex)_{0.7}Sr_{0.3}MnO_3$ ($0\leq x\leq 0.20$) perovskite, Ceramics International'(2015) 41:1929–1936

[15] E.Barsoukov and J R Macdonald Impedance spectroscopy (New York: Wiley) (2005) Chapter 4: 58.

[16] F. SallemiEmail author, M. Megdiche, B. Louati, K. Guidara, Electrical properties and complex impedance analysis of $K_2ZnV_2O_7$, Indian Journal of Physics, (2014) Volume 88, Issue 12: 1251–1256.

[17] N. Matsui, Complex-impedance analysis for the development of zirconia oxygen sensors, Solid State Ionics, (1981) 3–4: 525–529.

[18] L.Ding, Human University of Technology, mater science (2008) 25:4.